

Lawrence Berkeley Laboratory

UNIVERSITY OF CALIFORNIA

Physics, Computer Science & Mathematics Division

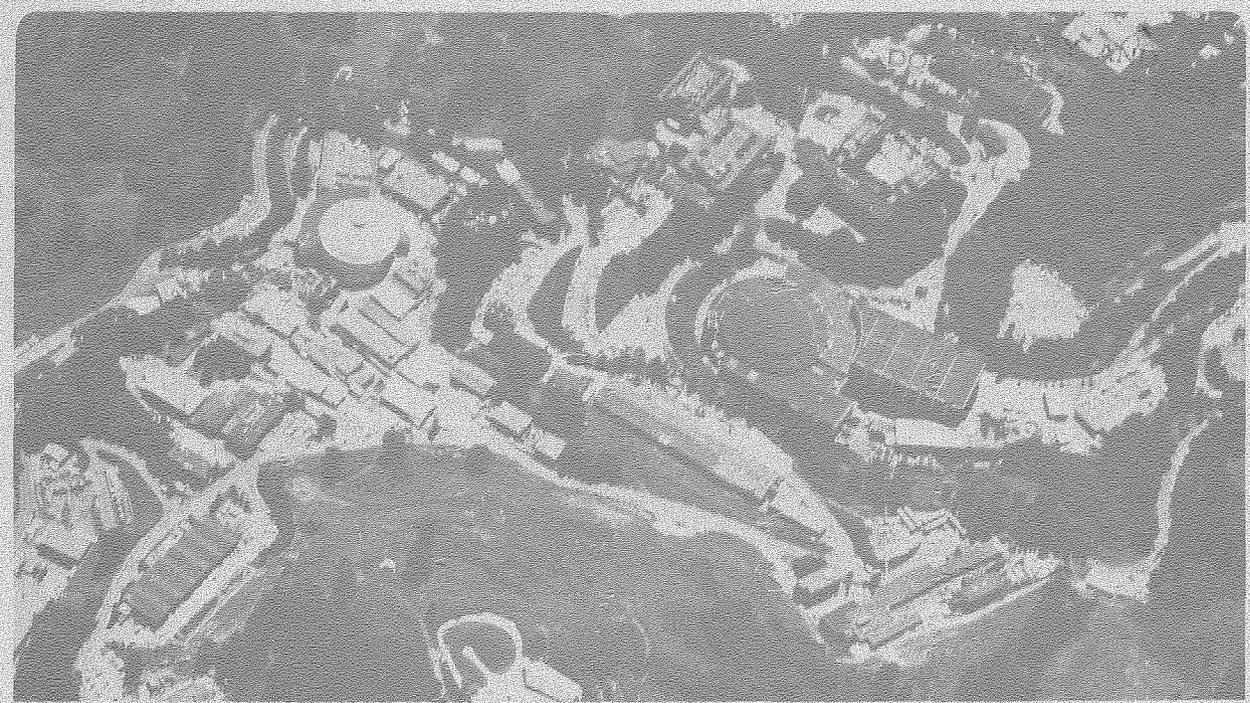
Submitted to Nuclear Physics B

HIGHER ORDER QCD CORRECTIONS TO DOUBLE MOMENT RATIOS IN DEEP INELASTIC SCATTERING

Jon Sheiman, Ian Hinchliffe, and H.E. Haber

September 1980

RECEIVED
LAWRENCE
BERKELEY LABORATORY
NOV 17 1980



LBL-11577 c.2

DISCLAIMER

This document was prepared as an account of work sponsored by the United States Government. While this document is believed to contain correct information, neither the United States Government nor any agency thereof, nor the Regents of the University of California, nor any of their employees, makes any warranty, express or implied, or assumes any legal responsibility for the accuracy, completeness, or usefulness of any information, apparatus, product, or process disclosed, or represents that its use would not infringe privately owned rights. Reference herein to any specific commercial product, process, or service by its trade name, trademark, manufacturer, or otherwise, does not necessarily constitute or imply its endorsement, recommendation, or favoring by the United States Government or any agency thereof, or the Regents of the University of California. The views and opinions of authors expressed herein do not necessarily state or reflect those of the United States Government or any agency thereof or the Regents of the University of California.

September 1980

LBL-11577

Section I

HIGHER ORDER QCD CORRECTIONS TO
DOUBLE MOMENT RATIOS IN DEEP INELASTIC SCATTERING

Jon Sheiman, Ian Hinchliffe, and H.E. Haber*

Lawrence Berkeley Laboratory
University of California
Berkeley, California 94720

Abstract

Order α^2 contributions to double moment ratios in semi-inclusive deep inelastic scattering are computed. They are substantial.

This paper is concerned with higher order QCD corrections to double moment ratios in deep-inelastic lepto-production. Before entering a discussion of the process in detail we will first make a few comments concerning such higher order QCD corrections* and ambiguities therein. Consider a process calculated through at least two orders in perturbation theory. For convenience write

$$P = A + B\alpha_s(\mu^2)$$

where A and B are the same order in $\alpha_s(\mu^2)$. B depends on several factors. If A contains the coupling constant $\alpha_s(\mu^2)$, B will depend on the renormalization scheme used to define α_s and on the scale μ at which it is evaluated.** In cases where the parton model (e.g. the Drell-Yan process [2]) is used and P is a parton process then B will depend on the scale at which the parton distributions are evaluated. A criterion for the validity of perturbation theory is $B\alpha_s \ll A$. Generally speaking if this criterion is satisfied then QCD is tested by fitting the data to the lowest order term A; few data are sufficiently accurate to be able to detect the presence of a small B term. If the criterion is not satisfied then the process is useless as a quantitative QCD test.

Unfortunately it is true that by appropriate choice of scheme and scale(s) it is almost always possible to satisfy the criterion. The decision on the status of perturbation theory then rests on

* Present address: Physics Department, University of Pennsylvania, Philadelphia, Pennsylvania 19174.

* For a relatively complete list of processes see Ref. [1].

** Strictly speaking the scheme and the scale μ are equivalent, however it is convenient to think of them as independent.

whether those schemes and scales are reasonable (or on a calculation to yet another order in α_s). Ideally one would like to have some a priori method of choosing schemes and scales in order to remove ambiguities in B. If this choice fails then the perturbation expansion would be meaningless. Unfortunately no such method exists rendering it extremely difficult to decide on the merits of ad hoc a posteriori choices which happen to make B small.

Three schemes are widely used, minimal subtraction (MS), mutilated minimal subtraction (\overline{MS}) [3] and momentum space subtraction [4]. The former is unphysical but there is no reason to prefer either of the other two, or indeed some other scheme. With regard to the scale of μ^2 , if the process is characterized by only one physical scale Q^2 , then it seems natural to choose $\mu^2 = Q^2$. But who is to say that $2Q^2$ or $Q^2/2$ is unreasonable? In processes with more than one physical scale such as large p_T hadron scattering [5] the situation is more complicated and ambiguous.

The outline of this paper is as follows: Section II contains a detailed discussion of the double moment ratios; Sections III and IV contain a discussion of the graphs we calculate; finally Section V contains our results and conclusions. We have elected not to give detailed formula. A presentation of them would not clarify this paper and would make it very long. We would be happy to supply a formula for the final answer to anyone who requests it; either on a roll of paper or on a stack of (400) fortran cards.

Section II

Consider one particle inclusive neutrino production:

$$W_\nu(q) + N(P_1) \rightarrow \pi(P_2) + X$$

where $W(q)$ is a virtual W meson of momentum q ($Q^2 \equiv -q^2 > 0$), N is a nucleon of momentum P_1 , and π is a pion of momentum P_2 . We will describe the process by the scaling variables x_h and z_h^*

$$x_h = \frac{Q^2}{2P_1 \cdot q}, \quad 0 \leq x_h \leq 1$$

$$z_h = \frac{P_1 \cdot P_2}{P_1 \cdot q}, \quad 0 \leq z_h \leq 1$$

and define the semi-inclusive "cross-section" as follows:

$$\frac{dW_h^{\mu\nu}(x_h, z_h, Q^2)}{dz_h} = \frac{1}{4\pi} \int \frac{d^3 P_2}{(2\pi)^{3/2} (2E_2)} \left[d^4 x e^{iq \cdot x} \delta\left(z_h - \frac{P_1 \cdot P_2}{P_1 \cdot q}\right) \right]$$

$$\int_X \langle P_1 | J^{\mu\dagger}(x) | P_2, X \rangle \langle P_2, X | J^\nu(0) | P_1 \rangle,$$

where J^μ is the charged weak current.

The QCD parton model relates the hadronic cross-section to the analogously defined partonic cross-section for the process

$$W^\nu(q) + \text{Parton}(P_1) \rightarrow \text{Parton}(P_2) + X.$$

With the definitions

$$x = \frac{Q^2}{2P_1 \cdot q}, \quad 0 \leq x \leq 1$$

$$z = \frac{P_1 \cdot P_2}{P_1 \cdot q}, \quad 0 \leq z \leq 1$$

* One could use the variable $\omega_h = \frac{-2P_2 \cdot q}{Q^2}$ instead of z_h . The former choice has the advantage of being insensitive to target mass effects [6]. We choose z_h because it compresses the fragmentation region (i.e. $P_2 \cdot P_1 = 0$) down to the single point $z_h = 0$. Thus moment integrals can extend through all of phase space, simplifying the calculation.

the relation is

$$\frac{dW_h(x_h, z_h, Q^2)}{dz_h} = \int_{x_h}^1 \frac{dx}{x} \int_{z_h}^1 \frac{dz}{z} F\left(\frac{x_h}{x}\right) \frac{dW(x, z, Q^2)}{dz} D\left(\frac{z_h}{z}\right). \quad (2.1)$$

In this equation, dW/dz is the partonic cross-section, F is the partonic distribution function of the nucleon, and D is the decay function of the final parton into the observed pion. We have dropped the usual sum over parton types on the assumption that non-singlet differences have been taken for both the nucleon and the pion. The Lorentz indices have been dropped on the assumption that a structure function has been projected out (see later).

Taking moments of Eq. (2.1) with respect to x_h and z_h gives

$$\left(\frac{dW_h}{dz_h}\right)^{(n,m)} \equiv F^{(n)} \left(\frac{d\tilde{W}}{dz}\right)^{(n,m)} D^{(m)}, \quad (2.2)$$

where

$$\left(\frac{dW_h}{dz_h}\right)^{(n,m)} \equiv \int_0^1 dx_h x_h^{n-1} \int_0^1 dz_h z_h^{m-1} \frac{dW_h}{dz_h}$$

and

$$\left(\frac{F}{D}\right)^{(P)} = \int_0^1 dU U^{P-1} \left(\frac{F(U)}{D(U)}\right).$$

The factorization theorem [7] guarantees that the infrared* (IR) singularities of dW/dz can be factored out and absorbed into a redefinition of F and D . The factorization takes the following form in moment space:

$$\left(\frac{dW}{dz}\right)^{(n,m)} = \Gamma^{(n)} \left(\frac{d\tilde{W}}{dz}\right)^{(n,m)} \Gamma^{(m)} \quad (2.3)$$

* We will consider the term "infrared singularities" to mean both soft and collinear divergences.

where all of the IR singularities of the right hand side reside in $\Gamma^{(n)}$ and $\Gamma^{(m)}$.

Performing IR renormalizations of F and D as follows

$$\begin{aligned} \tilde{F}^{(n)} &\equiv F^{(n)} \Gamma^{(n)}, \\ \tilde{D}^{(m)} &\equiv D^{(m)} \Gamma^{(m)}, \end{aligned}$$

Eq. (2.2) takes the manifestly finite form

$$\left(\frac{dW_h}{dz_h}\right)^{(n,m)} = \tilde{F}^{(n)} \left(\frac{d\tilde{W}}{dz}\right)^{(n,m)} \tilde{D}^{(m)}. \quad (2.4)$$

The zeroth order graph for dW/dz has a single particle final state, so by kinematics

$$\frac{dW}{dz} = \frac{d\tilde{W}}{dz} + O(\alpha_s) = A\delta(1-x)\delta(1-z) + O(\alpha_s).$$

Thus

$$\left(\frac{d\tilde{W}}{dz}\right)^{(n,m)} = A + O(\alpha_s)$$

and from Eq. (2.4)

$$\left(\frac{dW_h}{dz_h}\right)^{(n,m)} = A\tilde{F}^{(n)}\tilde{D}^{(m)} + O(\alpha_s). \quad (2.5)$$

The zeroth order result thus factorizes into a product of a function of n and a function of m .

Sakai [8] has invented a double moment ratio whose deviation from unity measures the breaking of this factorization:

$$R_S^{(n,m;l,k)}(Q^2) = \frac{\left(\frac{dW_h}{dz_h}\right)^{(n,m)} \left(\frac{dW_h}{dz_h}\right)^{(l,k)}}{\left(\frac{dW_h}{dz_h}\right)^{(n,k)} \left(\frac{dW_h}{dz_h}\right)^{(l,m)}}.$$

The QCD parton model prediction for R_S is, from Eq. (2.4) and Eq. (2.5)

$$R_S^{(n,m;l,k)} = \frac{\left(\frac{d\tilde{W}}{dz}\right)^{(n,m)} \left(\frac{d\tilde{W}}{dz}\right)^{(1,k)}}{\left(\frac{d\tilde{W}}{dz}\right)^{(n,k)} \left(\frac{d\tilde{W}}{dz}\right)^{(1,m)}} \quad (2.6)$$

From Eq. (2.3), this can also be written as

$$R_S^{(n,m;l,k)} = \frac{\left(\frac{dW}{dz}\right)^{(n,m)} \left(\frac{dW}{dz}\right)^{(1,k)}}{\left(\frac{dW}{dz}\right)^{(n,k)} \left(\frac{dW}{dz}\right)^{(1,m)}} \quad (2.7)$$

Of course, the IR singularities in Eq. (2.7) must cancel, since Eq. (2.6) gives R_S as a manifestly finite quantity.

The essential property of R_S is that the distribution and decay functions cancel out of it. Indeed, from Eq. (2.7) we see that the prediction for R_S takes the form of a power series in $\alpha_S(\mu)$ with calculable numerical coefficients. The coefficients depend on $\frac{\mu^2}{Q^2}$, where μ is the ultraviolet (UV) renormalization point, and on the UV renormalization scheme.* The only phenomenological input necessary is the value of α_S at some point. Thus, in terms of phenomenology and theoretical ambiguity R_S is analogous to R in e^+e^- annihilation [9].

R_S is an especially interesting quantity with which to investigate the behavior of perturbation theory. The freedom to define away higher order corrections is limited by the fact that there is only one kinematic scale in the process (Q), and only one theoretical

* All dependence on the IR renormalization scheme drops out in the ratio.

choice to make (the choice of a coupling constant). Furthermore, one of the usual ways to "improve" a badly converging perturbation series is to pull out π^2 's on the assumption that they factor off into exponentials to all orders. Any such terms would cancel out of R_S . Thus a large correction to R_S for a reasonable choice of a coupling constant indicates a deeper problem.

The fact that R_S can be expressed directly in terms of partonic cross-sections (see Eq. (1.7)) simplifies the calculation enormously, since we never have to factor the IR singularities. The factorization requires calculation of all of the graphs contributing to dW/dz and careful treatment of the IR singularities as x or z approach unity.

The use of Eq. (2.7) saves us much of this trouble. Consider dW/dz to the 4th order

$$\frac{dW}{dz} = A \left[\delta(1-x)\delta(1-z) + \frac{\alpha_S}{4\pi} d(x,z) + \left(\frac{\alpha_S}{4\pi}\right)^2 e(x,z) + \dots \right]$$

In terms of moment

$$\left(\frac{dW}{dz}\right)^{(n,m)} = A \left[1 + \frac{\alpha_S}{4\pi} d^{(n,m)} + \left(\frac{\alpha_S}{4\pi}\right)^2 e^{(n,m)} + \dots \right]$$

Thus Eq. (2.7) becomes

$$\begin{aligned}
R_S^{(n,m;l,k)} &= 1 + \left(\frac{\alpha_S}{4\pi}\right) \left[d^{(n,m)} + d^{(l,k)} - d^{(n,k)} - d^{(l,m)} \right] \\
&+ \left(\frac{\alpha_S}{4\pi}\right)^2 \left[\frac{1}{2} \left[d^{(n,m)} + d^{(l,k)} - d^{(n,k)} - d^{(l,m)} \right]^2 \right. \\
&\quad \left. - \frac{1}{2} \left[\left(d^{(n,m)} \right)^2 + \left(d^{(l,k)} \right)^2 \right. \right. \\
&\quad \left. \left. - \left(d^{(n,k)} \right)^2 - \left(d^{(l,m)} \right)^2 \right] \right] \\
&+ \left(\frac{\alpha_S}{4\pi}\right)^2 \left[e^{(n,m)} + e^{(l,k)} - e^{(n,k)} - e^{(l,m)} \right] \\
&+ O\left(\alpha_S^3\right)
\end{aligned} \tag{2.8}$$

Note that the contribution of the 4th order graphs (i.e. $e(x,z)$) to

R_S is

$$\left(\frac{\alpha_S}{4\pi}\right)^2 \int_0^1 dx \int_0^1 dz \left[(x^{n-1} - x^{l-1})(z^{m-1} - z^{k-1}) \right] e(x,z) + O(\alpha_S^3) . \tag{2.9}$$

Thus any singularity in $e(x,z)$ at x or z near 1 is controlled by the moment weighting in square brackets, and therefore requires no special treatment. Furthermore the two loop graphs (e.g. Fig. 2) which are all proportional to $\delta(1-x)\delta(1-z)$ make no contribution to 4th order.

We conclude this section by listing further simplifications and assumptions made in our calculation.

In order to simplify the Dirac algebra we consider the structure function which is obtained by contracting the Lorentz indices of the

W's.* Note that this choice eliminates interference between the vector and axial vector weak currents. Thus we did not have to worry about regulating IR divergences in the presence of a γ_5 . We take a strong isospin non-singlet, charge conjugation odd difference for the final state (i.e. $\pi^+\pi^-$). The relevant linear combination of final state partons is therefore $u-d-\bar{u}+\bar{d}$.

For the initial state, we also take a non-singlet difference (e.g. proton-neutron). To fix the relative contributions of quarks and antiquarks in the initial state, we take the Cabbibo angle to be zero. The G parity** of J_V and J_A (1 and -1 respectively) guarantees that quarks and antiquarks contribute with opposite signs.

Thus we compute the following sum

$$\frac{dW}{dz} \equiv \frac{dW_{d \rightarrow u}}{dz} + \frac{dW_{u \rightarrow d}}{dz} - \frac{dW_{d \rightarrow d}}{dz} - \frac{dW_{u \rightarrow u}}{dz} - \left(\frac{dW_{\bar{d} \rightarrow \bar{u}}}{dz} + \frac{dW_{\bar{u} \rightarrow \bar{d}}}{dz} - \frac{dW_{\bar{d} \rightarrow \bar{d}}}{dz} - \frac{dW_{\bar{u} \rightarrow \bar{u}}}{dz} \right) .$$

The terms with initial antiquarks simply reproduce the above sum by G parity.

Section III

We calculate the graphs which contribute to the cross-section with two body final states (virtual graphs) in this section. The graphs are computed in the Euclidean region where $x > 1$ and there are no discontinuities. Analytic continuation then yields the

* In the notation of Ellis [10] this corresponds to the combination

$$-3W_1 + \frac{v^2}{2Q_M^2} W_2 .$$

** The G parity we need here consists of a weak isospin rotation by π followed by charge conjugation.

correct result in the physical region $0 < x < 1$. All the calculations are performed in Feynman gauge. Dimensional regularization is used to control both the UV and IR divergences [11]. Integrals are performed in n dimensions and the singularities associated with UV and IR divergences appear as poles in $\epsilon(n = 4 - 2\epsilon)$. If UV subtraction is necessary then it is important to distinguish between the UV and IR poles so that the former can be subtracted. This can always be done by first evaluating the graph with the external legs off shell, extracting the UV poles, and then taking the on shell limit when the IR poles appear. However with the use of Feynman parameters the UV and IR singularities are always distinct. The former appear in momentum integrals and the latter in Feynman parameter integrals.

The order α_s contribution to $\frac{dW}{dz}$, $\left[d(x,z) \right]$, is obtained from Figs. 3(a), 3(b), and 3(c). Figure 3(a) gives a contribution proportional to $\delta(1-z) \delta(1-x)$ which cancels from R_s to this order. Figs. 3(b) and 3(c) give

$$d(x,z) = \frac{8}{3} \frac{2(1-x-z) + (x+z)^2}{(1-x)(1-z)} + O(\epsilon)$$

Before considering the order α^2 virtual graphs proper let us first dispose of the order α^2 contributions to R_s coming from the order α contributions. $(d^{mn} + d^{kl} - d^{nk} - d^{ml})^2$ is IR finite since it is simply the square of the order α piece. However the term $(d^{nm})^2 + (d^{lk})^2 - (d^{nk})^2 - (d^{lm})^2$ contains IR singularities which cancel against those from the order α^2 graphs (e^{mn} etc.). In order to obtain the cancellation before integration over x and z it is sufficient to notice that

$$(d^{mn})^2 = \int x^{m-1} z^{n-1} (d \circ d) dx dz$$

where

$$d \circ d(x,z) = \int_x^1 \frac{dx}{x} \int_z^1 \frac{dz}{z} d(\bar{x}, \bar{z}) d\left(\frac{x}{\bar{x}}, \frac{z}{\bar{z}}\right)$$

and $d(x,z)$ comes from the order α graphs shown in Fig. 3. This convolution is easily performed. Note that the virtual graph Fig. 3(a) which did not contribute to the order α piece of R_s must now be included in the convolution. It is important that $d(x,z)$ be retained in n dimensions until after the convolution has been performed when a Laurent expansion about $\epsilon = 0$ reveals double and single IR poles. The order α^2 piece of R_s can now be written as

$$\begin{aligned} & \left(\frac{\alpha_s}{4\pi}\right)^2 \int dx dz (x^{n-1} - x^{l-1}) (z^{m-1} - z^{k-1}) \left[e(x,z) - \frac{1}{2} d \circ d \right] \\ & + \frac{1}{2} \left(\frac{\alpha_s}{4\pi}\right)^2 \left[d^{mn} + d^{kl} - d^{nk} - d^{ml} \right]^2 \end{aligned} \quad (3.1)$$

We now turn to the virtual diagrams contributing to $e(x,z)$.

The first set of such graphs consists of the one loop corrections to the vertices and propagators in Figs. 3(b) and 3(c). The corrections to the external quark lines and the W-quark vertex can be considered together. A Ward identity ensures that the UV divergences arising from these graphs will cancel so that it is not necessary to perform a UV subtraction on them. This is especially convenient since the unsubtracted self energy of an on shell massless fermion is zero in dimensional regularization.

The corrections to the internal (off shell) fermion lines, external gluon lines and gluon vertices need UV subtractions. We must specify the subtraction scheme and hence the coupling constant. We use the \overline{MS} scheme [3] which entails subtracting the UV poles

as well as attendant Euler numbers and $\log(4\pi)$. Momentum space subtraction will be briefly mentioned later. After performing the subtractions all the remaining integrals are straightforward; no function worse than a \log^2 appears.

The most difficult virtual diagrams are the box graphs shown in Fig. 4. These graphs have no UV singularities but contain single and double IR poles. The integrals are complicated by the need to retain these terms as well as ϵ^0 terms. Some comments on our technique may prove useful elsewhere. It is convenient to delay integrals over loop momenta until after forming the cross-section by multiplying by the lower order graphs and performing the Dirac algebra. Feynman parameters are introduced and the loop momentum integral performed. This leaves Feynman parameter integrals of the following type

$$I_P = \int_0^1 d\alpha_1 \int_0^{1-\alpha_1} d\alpha_2 \int_0^{1-\alpha_2-\alpha_1} d\alpha_3 \frac{f(\alpha_1, \alpha_2, \alpha_3)}{[A\alpha_2(1-\alpha_2-\alpha_3) + B\alpha_1(\alpha_2+\alpha_3) + C\alpha_1\alpha_2]^P},$$

where A, B, and C are scalar products of various combinations of external momenta and f is a polynomial. There are 17 such integrals with $p = 2 + \epsilon$ and 4 with $p = 1 + \epsilon$. These can be simplified and reduced in number as follows:

change variables

$$\begin{aligned} uv &= \alpha_2, \\ u(1-v) &= \alpha_3, \\ x(1-u) &= \alpha_1; \end{aligned}$$

then

$$I_P = \int_0^1 u^{1-P} (1-u)^{1-P} du \int_0^1 dv \int_0^1 \frac{dx f(x, u, v)}{(Av + Bx + Cxv)^P}.$$

Since f is a polynomial the integral over u is trivial. The following integral now remains

$$\int_0^1 dv \int_0^1 \frac{dx g(x, v)}{(Av + Bx + Cxv)^P},$$

where g is a polynomial. All integrals of this type can be gotten from

$$J_P = \int_0^1 dv \int_0^1 \frac{dx}{(Av + Bx + Cxv)^P},$$

by differentiation with respect to different combinations of A, B, and C.

$$J_P = \frac{1}{(2-P)(1-P)AB} \left(\frac{AB}{C}\right)^{2-P} \left[-F\left(P, -\frac{C(A+B+C)}{AB}\right) + F\left(P, -\frac{C}{A}\right) + F\left(P, -\frac{C}{B}\right) \right]$$

with $F(P, x) = x^{2-P} {}_2F_1(1, 2-P, 3-P, x)$ and ${}_2F_1(a, b, c, x)$ is the usual hypergeometric function. We need J_P for $P = -1 + \epsilon$, ϵ , $1 + \epsilon$, and $2 + \epsilon$. The extra values of P arise because of the need for differentiation. It is necessary to expand these functions in power series about $\epsilon = 0$. The relevant expansions are

$$\begin{aligned} {}_2F_1(1, -\epsilon, 1-\epsilon, x) &= 1 + \epsilon \ln(1-x) - \epsilon^2 \text{Li}_2(x) \\ {}_2F_1(1, 1-\epsilon, 2-\epsilon, x) &= \frac{(1-\epsilon)}{x} \left[-\ln(1-x) + \epsilon \text{Li}_2(x) + \epsilon^2 \text{Li}_3(x) \right] \end{aligned}$$

$${}_2F_1(1, 2-\epsilon, 3-\epsilon, x) = \frac{(2-\epsilon)}{x^2} \left[-\ln(1-x) - x + \epsilon \left(\text{Li}_2(x) - x \right) + \epsilon^2 \left(\text{Li}_3(x) - x \right) \right]$$

$${}_2F_1(1, 3-\epsilon, 4-\epsilon, x) = \frac{(3-\epsilon)}{x^3} \left[-\ln(1-x) - x - \frac{x^2}{2} + \epsilon \left(\text{Li}_2(x) - \frac{x^2}{4} - x \right) \right]$$

and $\text{Li}_n(x) = \sum_{p=0}^{\infty} \frac{x^p}{p^n}$ is the usual polylogarithm [12]. Although trilogarithms appear in these expansions they are absent from the final result for the box graphs which does however contain some 17 dilogarithms.

Section IV

In this section, we discuss the graphs with three body final states.

The graphs contributing to a 2 gluon, 1 quark final state are shown in Fig. 5. The diagrams are drawn as squared amplitudes. The lines crossing the cut are the unobserved partons. One must take care not to sum over the (unphysical) longitudinal polarization of the final gluons. This presents no problem when there is only one external gluon, but when there are two, the full spin sum operator

$$\sum_{\substack{\text{physical} \\ \text{polarization} \\ \lambda}} e^{*\alpha}(P, \lambda) e^{\beta}(P, \lambda) = - \left[g^{\alpha\beta} - \frac{P^{\alpha}\bar{P}^{\beta} + P^{\beta}\bar{P}^{\alpha}}{P \cdot \bar{P}} \right]$$

$$P = (E, \vec{P}) \quad , \quad \bar{P} = (E, -\vec{P})$$

must be used on one of the gluons. The usual sum over physical and non-physical polarizations may then be used on the other one, by the

Ward identities. Note that since either of the gluons crossing the cut in Fig. 5 may be the "special" one, we must average over both possibilities. It is convenient to label the cut momenta so that only one non-covariant vector \bar{P} appears. The Dirac algebra can be reduced by using the interchange $P_1 \leftrightarrow -P_2$ to generate graphs from each other (e.g. Figs. 5(a) and 5(f) are related by this interchange). When the results were added up, the vector \bar{P} dropped out.

We can use arguments involving flavor to discard many of the graphs contributing to a 3 fermion final state. For instance, Fig. 6(a) and Fig. 6(b) each are zero because the charged weak current changes flavor.* Figure 6(c) vanishes due to the non-singlet sum on the final observed quark.

The remaining graphs are divided by their flavor-topological structure into Figs. (7 → 13).

Table I lists the processes to which each class contributes (assuming an incoming W^+ boson), and the associated weight from Eq. (2.10) (of course this weight is the same for a W^- by G parity). Also listed is the factor (if any) which arises from the sum over the flavors of the unobserved fermions. N_f is the number of quark flavors.

A careful application of Wick's theorem shows that Figs. (9 → 13) all receive Fermi minus signs.

We have indicated the usefulness of interchanging Fermion momenta to generate graphs from each other. Numerous such transformation exist involving the graphs with 3 final state fermions. The Dirac algebra for Figs. 7 and 8 can be generated from

* These graphs do contribute to R_s in electroproduction.

Figs. 7(a) and 7(b). Similarly Figs. 9-13 can be generated from Figs. 9(a)-9(c).

We now describe the phase space integrals for the real emission graphs. Let P_3 and P_4 be the momenta of the unobserved partons. For fixed P_1 and P_2 , $P_3 + P_4$ is fixed by momentum conservation. The remaining integral over the unobserved momenta is performed in their center of mass frame (which is the usual Gottfried-Jackson (GJ) frame), i.e.

$$\vec{P}_3 + \vec{P}_4 = \vec{P}_1 + \vec{q} - \vec{P}_2 = 0 \quad (4.1)$$

We further define

$$y \equiv \frac{x \left[z + \frac{2P_2 \cdot q}{Q^2} \right]}{(1-x)(1-z)} \quad 0 \leq y \leq 1$$

Then the 3 body phase space integral is

$$\begin{aligned} & \frac{1}{4\pi} \int \frac{d^{n-1} \vec{P}_2}{(2\pi)^{\frac{n-1}{2}} (2E_2)} \delta \left(z - \frac{P_1 \cdot P_2}{P_1 \cdot q} \right) \int \frac{d^{n-1} \vec{P}_3}{(2\pi)^{\frac{n-1}{2}} (2E_3)} \int \frac{d^{n-1} \vec{P}_4}{(2\pi)^{\frac{n-1}{2}} (2E_4)} \\ & \times (2\pi)^n \delta^{(n)}(P_1 + q - P_2 - P_3 - P_4) |M|^2 \\ & = \frac{1}{2\Gamma(1-\epsilon)} \frac{1}{(4\pi)^{5-3\epsilon}} \left[\frac{z(1-x)^2(1-z)^2}{x^2} \right]^{-\epsilon} \\ & \cdot \int_0^1 dy y^{-\epsilon} (1-y)^{-\epsilon} \int d\Omega_{GJ} |M|^2 \quad (4.2) \end{aligned}$$

where $|M^2|$ is a squared matrix element, and $\int d\Omega_{GJ}$ is the angular integral of \hat{P}_3 ($= -\hat{P}_4$) over the $n-2$ dimensional sphere in the GJ frame.

Equation (4.1) implies that $\vec{P}_1 \cdot \vec{q}$ and \vec{P}_2 span a 2 dimensional plane; call it the xz plane. Introduce angles θ and ϕ such that

$$\begin{aligned} (\vec{P}_3)_z &= E_3 \cos\theta \quad , \quad 0 \leq \theta \leq \pi \\ (\vec{P}_3)_x &= E_3 \sin\theta \cos\phi \quad , \quad 0 \leq \phi \leq \pi \end{aligned}$$

Then

$$d\Omega_{GJ} = d(\cos\theta) (1-\cos^2\theta)^{-\epsilon} d\phi (\sin\phi)^{-2\epsilon} (4\pi)^{-\epsilon} 2 \frac{\Gamma(1-\epsilon)}{\Gamma(1-2\epsilon)} \quad (4.3)$$

The angular integrals are performed by partial-fractioning the integrand. The resulting integrals are performed analytically as Laurent expansions in ϵ , keeping only terms which become order ϵ^0 or lower after the y integration (as we shall see, the y integration can introduce a factor of $\frac{1}{\epsilon}$). There were 4 basic types of integrals. Integrals of the type

$$I_1 = \int d\Omega_{GJ} \frac{1}{1-\hat{P}_3 \cdot \hat{V}} \quad \hat{V} = \pm \hat{P}_1, \pm \hat{P}_2$$

have singularities when $\hat{P}_3 = \hat{V}$.^{*} These poles are regulated by the Jacobian in Eq. (4.3); giving rise to a simple pole in ϵ .

Integrals of the form

$$I_2 = \int d\Omega_{GJ} \frac{1}{1-\vec{L} \cdot \hat{P}_3} \quad L \equiv |\vec{L}| \leq 1$$

arise from propagators of the form $1/(P_1 - P_2 - P_3)^2$. $L = 1$ can occur only when $P_1 \cdot P_2 = 0$, i.e. $z = 0$. Thus the $L = 1$ singularity requires no special treatment since it is removed by the moment weighting in Eq. (2.9). I_1 and I_2 are straightforward, and the results are

^{*} The symbol $\hat{}$ denotes a unit vector.

$$I_1 = \left[-\frac{1}{\epsilon} \right] (2\pi)(4\pi)^{-\epsilon} \frac{\Gamma(1-\epsilon)}{\Gamma(1-2\epsilon)}$$

$$I_2 = (2\pi)(4\pi)^{-\epsilon} \frac{\Gamma(1-\epsilon)}{\Gamma(1-2\epsilon)} \frac{1}{L} \left[\log \frac{1+L}{1-L} + A \right] + O(\epsilon^2)$$

where

$$A = -\frac{\epsilon}{2} \log^2 \left[\frac{1+L}{1-L} \right] + 2\epsilon \text{Li}_2 \left[\frac{-2L}{1-L} \right]$$

Integrals of the form

$$I_3 = \int_{\text{GJ}} d\Omega \frac{1}{(1-\hat{P}_3 \cdot \hat{V})(1-\hat{P}_3 \cdot \hat{L})}$$

can be performed by combining the denominators using Feynman parameters.

The result is

$$I_3 = \left[-\frac{1}{\epsilon} \right] (4\pi)^{1-\epsilon} \frac{\Gamma(1-\epsilon)}{2\Gamma(1-2\epsilon)} \left[1 + \epsilon \ln \left(\frac{1-L^2}{(1-\vec{L} \cdot \hat{V})^2} \right) \right] + \frac{\epsilon \vec{A} \cdot \hat{V}}{1-\vec{L} \cdot \hat{V}}$$

Finally, we had integrals of the form

$$I_4 = \int_{\text{GJ}} d\Omega \frac{1}{(1-\hat{P}_3 \cdot \hat{V})(1-\hat{P}_3 \cdot \hat{W})} \quad \begin{matrix} \hat{V} = \pm \hat{P}_1 \\ \hat{W} = \pm \hat{P}_2 \end{matrix}$$

The integrand has poles at $\hat{P}_3 = \hat{V}$ and at $\hat{P}_3 = \hat{W}$. As $\hat{V} \rightarrow \hat{W}$, the 2 singularities collide. This occurs when one of the following is satisfied*

$$\begin{matrix} \text{(case A)} & \hat{P}_1 = \hat{P}_2 \\ \text{(case B)} & \hat{P}_1 = -\hat{P}_2 \end{matrix}$$

* The A type singularities occur in Fig. 13 and Fig. 5(h)-5(k).

The B type occur in Figs. 5(b), 5(c), 5(d), 5(e), 5(o), and 5(p).

Kinematics dictates that case A occurs at $y = 1$, case B at $y = 0$.

Any Laurent expansion performed at this stage (i.e. before the y integration), must be uniform in y . Thus our expansion for I_4 must be uniform in $(\hat{V} \cdot \hat{W})$. This integral is performed in Ref. (5). The result is

$$I_4 = \left[-\frac{1}{\epsilon} \right] (4\pi)^{1-\epsilon} 2^\epsilon \frac{\Gamma(1-\epsilon)}{\Gamma(1-2\epsilon)} (1-x)^{-1-\epsilon} (1+\epsilon^2 \text{Li}_2(x))$$

where $x = \frac{(1-\hat{V} \cdot \hat{W})^2}{4}$. Since

$$\hat{P}_1 \cdot \hat{P}_2 = 1 + O(1-y), \quad \text{as } y \rightarrow 1$$

$$\hat{P}_1 \cdot \hat{P}_2 = -1 + O(y), \quad \text{as } y \rightarrow 0,$$

case A singularities result in singularities of the form $(1-y)^{-1-\epsilon}$ as $y \rightarrow 1$ similarly case B gives $y^{-1-\epsilon}$ as $y \rightarrow 0$.

The result of the angular integral as a function of y was complicated enough to prevent us from doing the y integral analytically. However, we still need to have the result as a Laurent expansion, even if the terms in it are integrals over y . We are prevented from simply expanding the integrand because of singularities of the form $(1-y)^{-1-\epsilon}$ as $y \rightarrow 1$ and $y^{-1-\epsilon}$ as $y \rightarrow 0$.* We handle these by the usual "plussing" technique, e.g.

* The colliding singularities of the angular integrals give rise to singularities of the form $(1-y)^{-1-2\epsilon}$ and $y^{-1-2\epsilon}$, the extra ϵ being due to the phase space factors of Eq. (4.2). Singularities of the form $(1-y)^{-1-\epsilon}$ also come from factors of

$$\frac{1}{(P_3 + P_4)^2} = \frac{x}{(1-x)(1-y)(1-z)}$$

$$(1-y)^{-1-\epsilon} = -\frac{1}{\epsilon} \delta(1-y) + \left(\frac{1}{1-y}\right)_+ - \epsilon \left(\frac{\log(1-y)}{1-y}\right)_+ + O(\epsilon^2)$$

and similarly for $y^{-1-\epsilon}$. This equation is valid when multiplying a function of y which is continuous at $y = 1$.

We have shown the great care with which the endpoint singularities in y must be handled. No such subtleties occur in the moment integration of Eq. (2.9) because the moment weighting cancels out all remaining endpoint singularities.

Section V

The IR singularities (i.e. poles and double poles in Eq. (2.8)) can now be assembled in the formula for R_s . Their contribution is given by the pole part of Eq. (3.1). The contribution of the real emission graphs to $e(x,z)$, discussed in the previous section is in the form of an integral over y . The integral is sufficiently simple that it can be performed analytically. The factorization theorem guarantees that R_s is IR finite for all moment indices. This can be true only if the integrand $e(x,z) - (d\odot d)/2$ is IR finite (up to delta functions at $x = 1$ or $z = 1$, which we have discarded). We verified explicitly that this was the case.

It now remains to evaluate the remaining integrals numerically in order to obtain values of R_s . The integral consists of two parts; a double integral over x and z coming from the IR finite parts of the graphs discussed in Sec. III and the parts from Sec. IV which result from the plussing operation; and a triple integral over the remaining terms from Sec. IV. These integrals are of course all finite, however they contain integrable singularities of the form $\log^2(1-x)$, $\log^2(1-z)$ etc. It is important to change variables to render these singularities

more amenable to numerical integration. The following variable transformation is very effective

$$\int_0^1 f(x) dx = \int_0^1 \frac{e^{1-1/y}}{y^2} f(e^{1-1/y}) dy$$

If $f(x) \sim \log^n(x)$ as $x \rightarrow 0$, the left hand side needs of order 500 steps to achieve a convergence on the integral, 10 steps are sufficient for the right hand side. The convergence of regular function integrals is unaffected by this variable change. Numerical integration of the (IR) finite parts of Eq. (2.8) is now simple and the results are displayed in Table II. Writing

$$R_s^{(n,m;l,k)} = 1 + A^{(n,m;l,k)} \left(\frac{\alpha_s(\mu^2)}{\pi} \right) + B^{(n,m;l,k)} \left(\frac{\alpha_s(\mu^2)}{\pi} \right)^2$$

the table shows values for A and B. It is clear that the corrections are large.

The numbers shown in the table are for the \overline{MS} scheme with $\mu^2 = Q^2$. The order α^2 terms are of the order of 60% of the order α terms for $\alpha = 0.2$. B is of course scheme dependent; in the momentum space scheme (Landau gauge) with $\mu^2 = Q^2$, B is given from the $B_{\overline{MS}}$ in the table by [4]

$$B_{\text{mom}} = B_{\overline{MS}} - 3.07 A \left(\frac{\alpha_s(\mu^2)}{\pi} \right)$$

Using a momentum space subtracted α therefore reduces the corrections to about 40%. The corrections get larger as the difference between n and l and k and m increases. This presumably reflects pieces of the formula for R_s which go like $\log^2(n)$ etc. Notice that the lowest

order term A is symmetric under the interchanges $m \leftrightarrow n$ and $k \leftrightarrow l$. This is a reflection of the fact that $d(x,z)$ is symmetric with respect to interchange of x and z . This symmetry is maintained in the B terms within the errors on our numerical integration. The fact that the ratio B/A is almost independent of the indices indicates that the corrections can be made uniformly small by using some fraction of Q^2 , as the scale in α_s . Unfortunately we need $Q^2/8$ in the momentum space scheme to make the α^2 term 10% of the α term. It seems difficult to see why this should be the correct scale although it is worth pointing out that within the momentum space scheme such a scale leads to reasonable (negative) corrections of the order of 20% to the usual formulae for the Q^2 evolution of moments in inclusive lepto-production. It can be argued [13] that a natural scale for μ^2 is $Q^2(1-z)(1-x)$; this scale being a typical off shell-ness of parton in the process. Now using this scale the lowest order contribution to R_s changes. Choosing the coupling constant such that $\alpha_s(100 \text{ GeV}^2) = 0.2$ Table III now shows the order α and order α^2 contributions to R . It is immediately clear that the corrections in order α^2 are now small, and the perturbation expansion appears to be reliable. Unfortunately to see that this is really the case needs a proof that such a choice of μ^2 will work to all orders in reducing the corrections. Such a proof is lacking, making it difficult to decide whether the smallness of the order α^2 terms is a mere coincidence.

In conclusion we have computed the order α_s^2 terms in the double moment ratio in semi-inclusive deep inelastic scattering. The corrections are large enough that one should worry about the status of the perturbation expansion. However they are not as large as those found in some other processes [14], and the fact that they depend only slightly on

the moment indices encourages one to think that something can be salvaged.

ACKNOWLEDGMENTS

This research was supported by the High Energy Physics Division of the U. S. Department of Energy under contract no. W-7405-ENG-48. All the algebraic manipulations in this paper were performed with the aid of MACSYMA [15]. We are grateful for the support provided by the MATHLAB group at MIT.

Graphs	Processes	Weight from Eq. (2.10)	Sum Over Unobserved Flavors
Fig. (7)	$\bar{d} \rightarrow \bar{u} + X$	1	N_f
Fig. (8)	$\bar{d} \rightarrow \bar{d} + X$ $u \rightarrow u + X$	-2	$\left[\frac{N_f}{2} \right]$
Fig. (9)	$\bar{d} \rightarrow \bar{u} + X$	1	1
Fig. (10)	$\bar{d} \rightarrow \bar{d} + X$ or $u \rightarrow u + X$	-1	1
Fig. (11)	$\bar{d} \rightarrow \bar{u} + X$	-1	1
Fig. (12)	$u \rightarrow \bar{d} + X$	-1	1
Fig. (13)	$\bar{d} \rightarrow \bar{d} + X$	1	1

TABLE I

List of flavor weights associated with Figs. 7-13.

n	m	l	k	A	B	% Correction ($\alpha = 0.2$)
2	2	3	3	0.204	1.78	55.5
2	2	3	4	0.344	3.13	57.8
2	2	3	5	0.453	4.22	59.3
2	2	3	8	0.680	6.731	62.9
2	2	4	5	0.767	7.50	62.2
2	2	5	5	1.01	10.22	64.3
2	2	6	6	1.45	15.4	67.7
2	2	10	10	3.10	39.2	80.3
2	3	3	4	0.141	1.32	59.9
2	3	3	5	0.249	2.39	61.2
2	3	4	5	0.423	4.21	63.4
2	3	5	6	0.756	7.90	66.5
2	4	3	5	0.108	1.055	62.0
2	4	5	5	0.243	2.50	65.3
3	3	4	4	0.0981	0.983	63.7
3	3	5	5	0.309	3.23	66.7
4	4	5	5	0.0588	0.637	68.8

TABLE II

Values of A and B in the formula.

$$R_s^{(n,m;l,k)} = 1 + A^{(n,m;l,k)} \left[\frac{\alpha_s(\mu^2)}{\pi} \right] + B^{(n,m;l,k)} \left[\frac{\alpha_s(\mu^2)}{\pi} \right]^2$$

in the \overline{MS} scheme with $\mu^2 = Q^2$.

n	m	l	k	LO	NLO	% Correction
2	2	3	3	0.013	0.00164	13
2	2	5	5	0.064	0.00947	15
2	2	10	10	0.197	0.043	21
2	4	3	5	0.0687	7.5×10^{-3}	11
3	3	5	5	0.0196	0.0023	12
4	4	5	5	0.0037	3.8×10^{-4}	10

TABLE III

Values of LO and NLO, and the percentage correction, in the formula $R_g = 1 + LO + NLO$, where LO is the lowest order contribution with $u^2 = Q^2(1-x)(1-z)$ in the \overline{MS} scheme (with $\alpha_{\overline{MS}}(Q^2) = 0.2$), and NLO is the next correction.

REFERENCES

- [1] C. H. Llewellyn Smith, talk given at the 20th International Conference on High Energy Physics, Madison, Wisconsin, July 1980.
- [2] G. Altarelli, R. K. Ellis and G. Martinelli, Nucl. Phys. B143 (1978) 521; (E: B146 (1978) 544); Nucl. Phys. B157 (1979) 461; J. Kubar-Andre and F. E. Paige, Phys. Rev. D19 (1979) 221.
- [3] W. A. Bardeen, A. J. Buras, D. W. Duke and T. Muta, Phys. Rev. D18 (1978) 3998.
- [4] W. Celmaster and R. J. Gonsalves, Phys. Rev. Letters 42, (1979) 1435 and Phys. Rev. D20, (1979) 1420. R. Barbieri et al., Phys. Letters 81B, (1979) 207.
- [5] R. K. Ellis, M. Furman, H. Haber, I. Hinchliffe, Lawrence Berkeley Laboratory Preprint LBL-10304 (to appear in Nucl. Phys. B); I. Hinchliffe, Lawrence Berkeley Laboratory Preprint LBL-11397, to appear in Proceedings of the 20th International Conference on High Energy Physics, Madison, Wisconsin, July 1980.
- [6] J. Sheiman, Nucl. Phys. B171 (1980) 445.
- [7] R. K. Ellis, H. Georgi, M. Machacek, H.D. Politzer, and G. C. Ross, Nucl. Phys. B152 (1979) 285; D. Amati, R. Petronzio and G. Veneziano, Nucl. Phys. B146 (1978) 29; A. H. Mueller, Phys. Rev. D18 (1978) 3705; S. B. Libby and G. Sterman, Phys. Rev. D18 (1978) 3252.
- [8] N. Sakai, Phys. Letters 85B (1979) 67.
- [9] M. Dine and J. Sapiirstein, Phys. Rev. Lett. 43 (1979) 668; K. G. Chetyrkin, A. L. Kataev and F. V. Tkachov, Phys. Lett. 85B (1979) 277.

- 10 J. Ellis, "Deep Hadronic Structure" in "Weak and Electromagnetic Interactions at High Energies," ed. R. Balian and C. H. Llewellyn Smith, (North Holland, 1977).
- 11 G. 't Hooft and M. Veltman, Nucl. Phys. B44 (1972) 189;
C. G. Bollini and J. J. Giambiagi, Nuovo Cim. 12B (1972) 20;
W. J. Marciano, Phys. Rev. D12 (1975) 3861.
- 12 L. Lewin, "Dilogarithms and Associated Functions," (MacDonald, London, 1958).
- 13 S. Brodsky and P. Lepage, SLAC Publication 2446.
- 14 R. K. Ellis, D. A. Ross and A. E. Terrano, CALT 68 785, see also Refs. [2] and [5].
- 15 MATHLAB Group, MIT Laboratory for Computer Science, "MACSYMA Primer," (March 1978) and "MACSYMA Reference Manual," Version 9 (December 1977).

FIGURE CAPTIONS

- Figure 1: The lowest order graph in semi-inclusive deep inelastic scattering.
- Figure 2: A two loop graph which does not contribute to R_S .
- Figure 3: Graph contributing to $\frac{dW}{dz}$ in order α_s .
- Figure 4: Virtual diagrams contributing to $\frac{dW}{dz}$ in order α_s^2 .
- Figure 5: Graphs contributing to $\frac{dW}{dz}$ with two gluons in the final state.
- Figure 6: Graphs which do not contribute to $\frac{dW}{dz}$ by virtue of their flavor structure.
- Figures 8-13: Graphs contributing to $\frac{dW}{dz}$ with one gluon and two fermions in the final state.

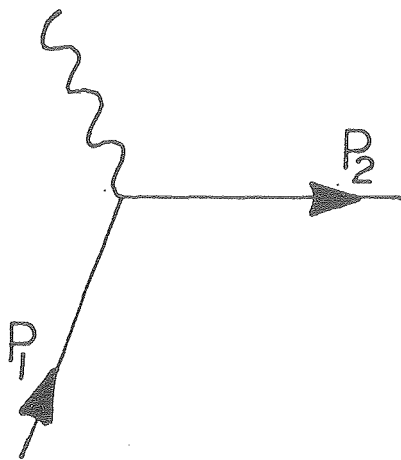


FIG. 1

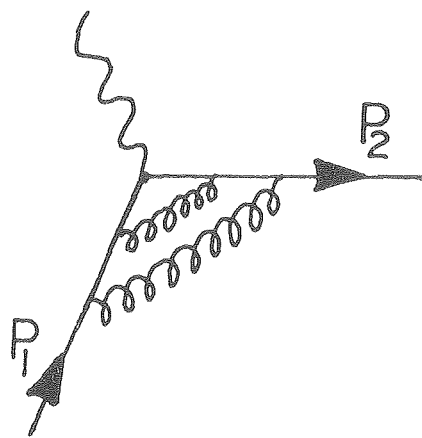
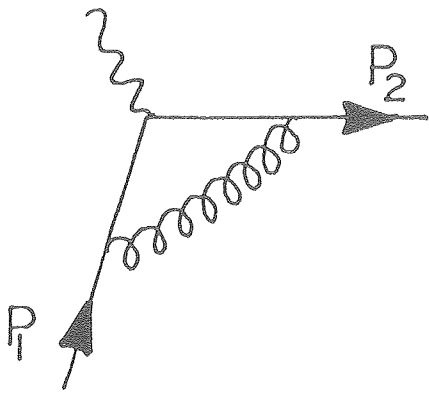
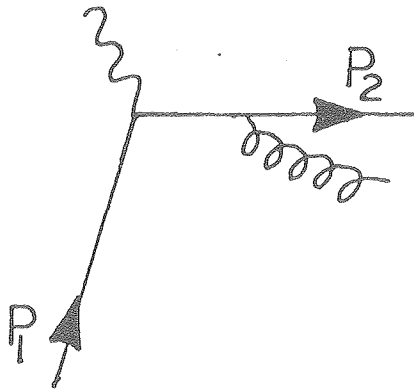


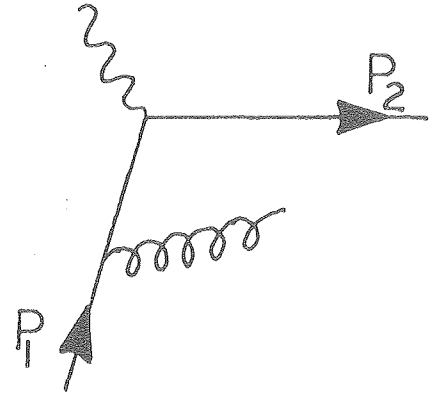
FIG. 2



(A)



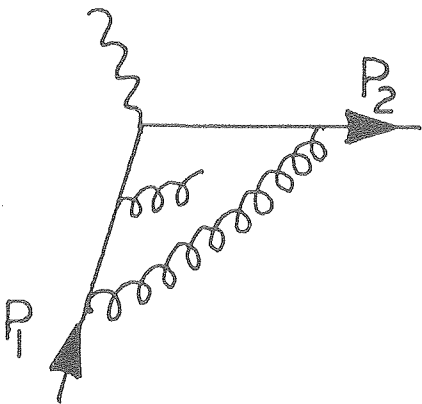
(B)



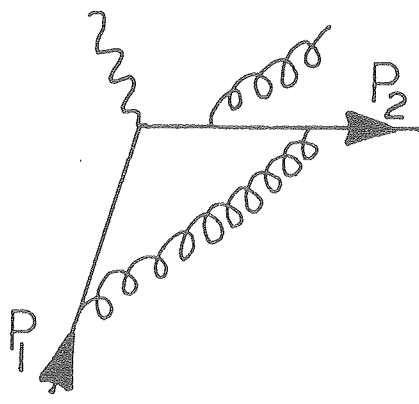
(C)

FIG. 3

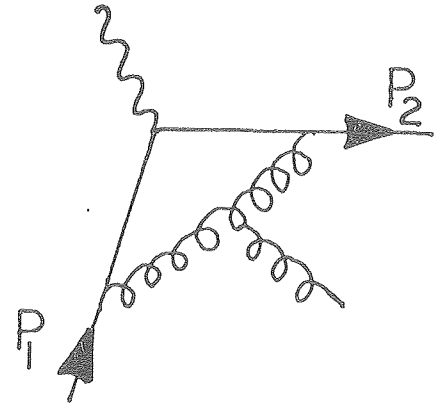
-32-



(A)

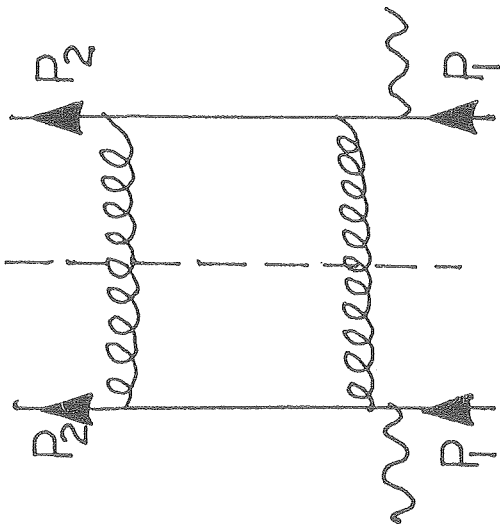


(B)

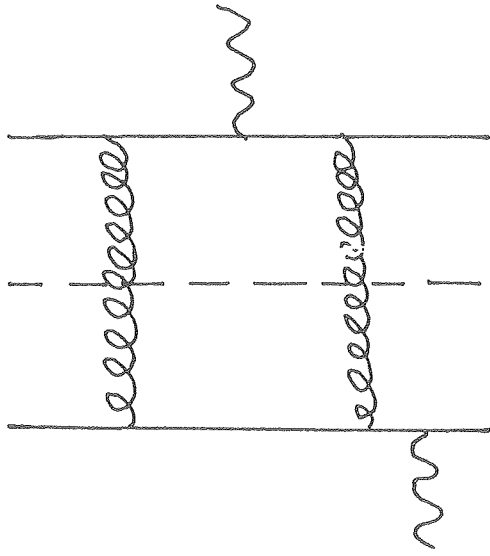


(C)

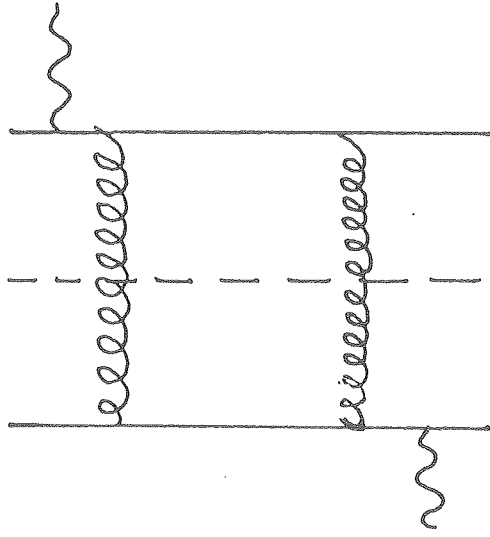
FIG. 4



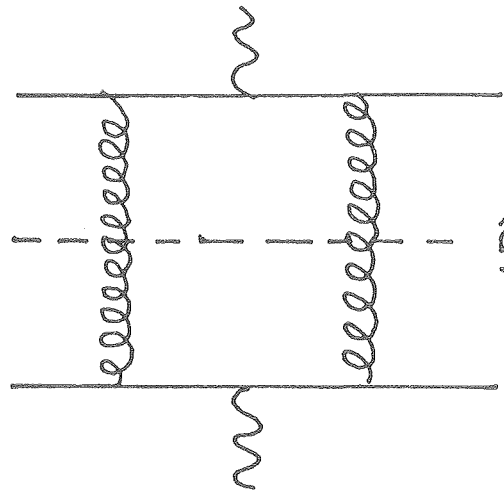
(A)



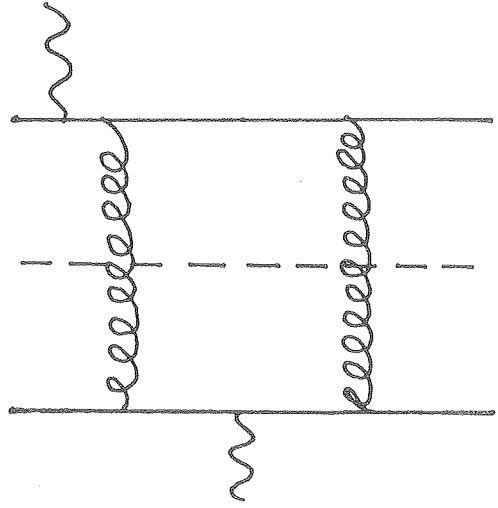
(B)



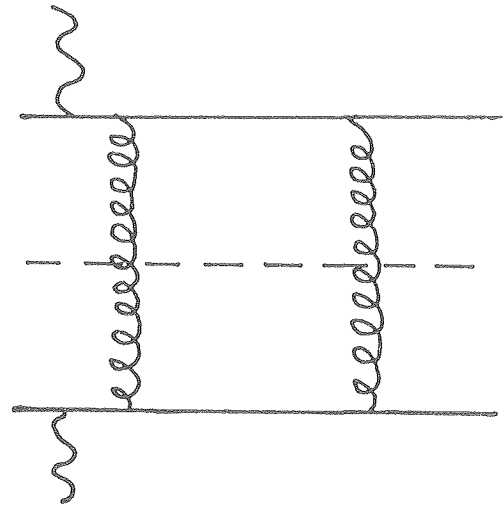
(C)



(D)



(E)



(F)

FIG. 5

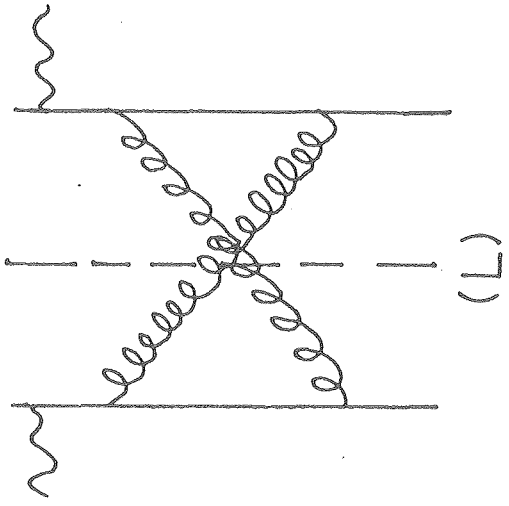
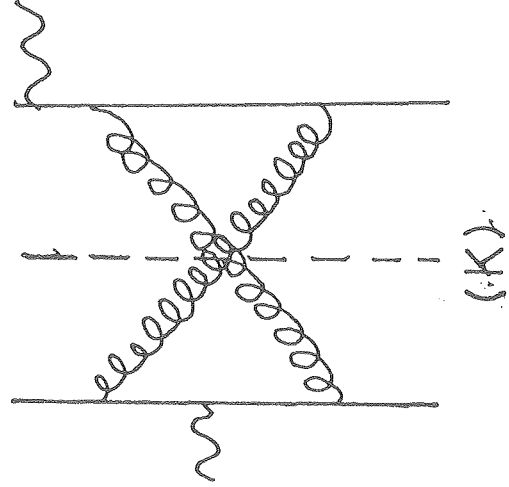
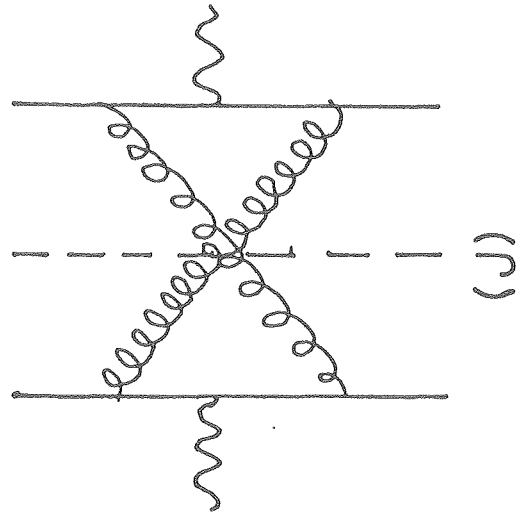
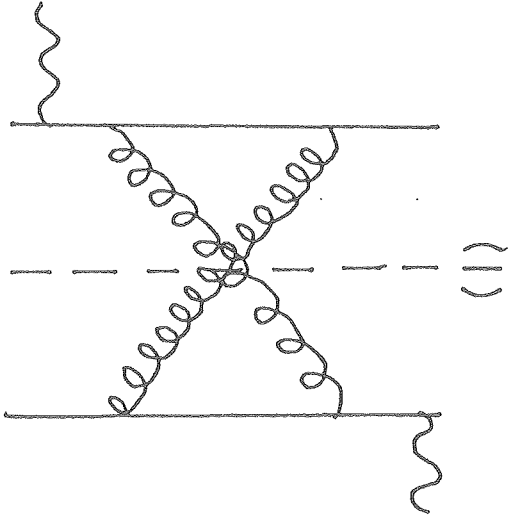
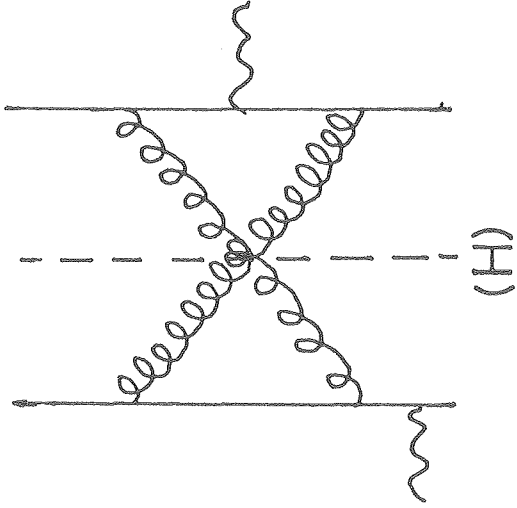
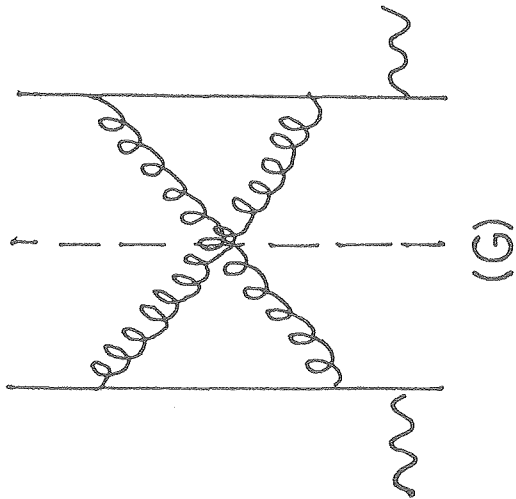


FIG. 5 (CONT.)

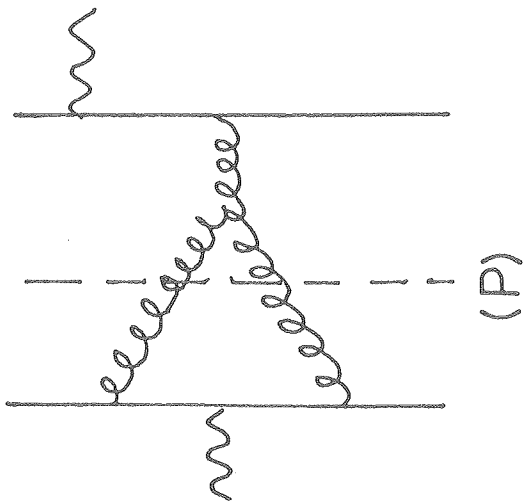
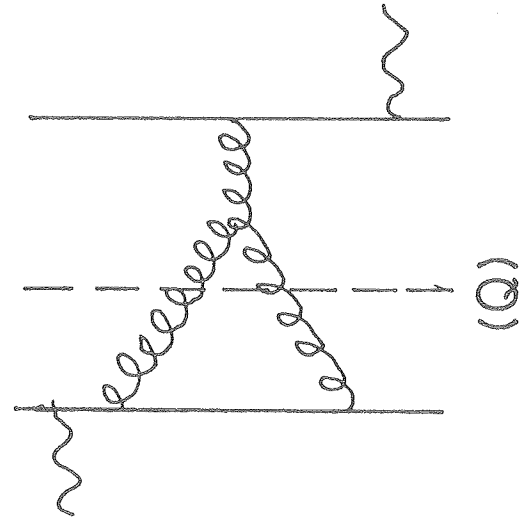
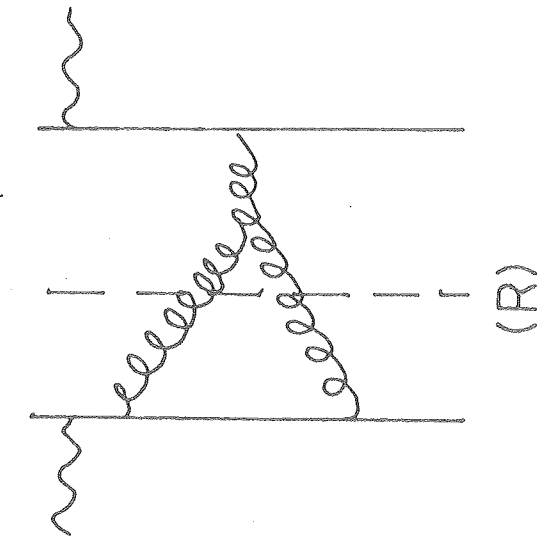
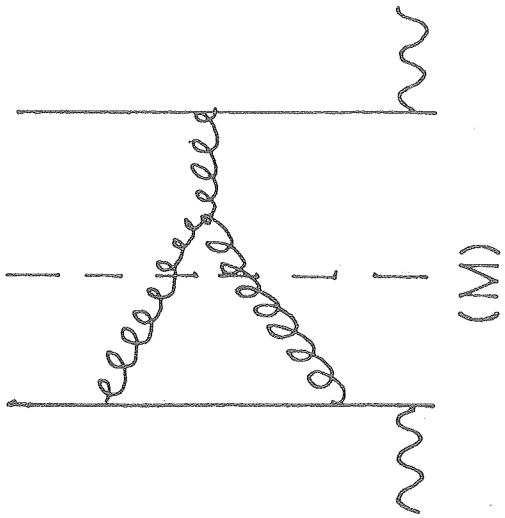
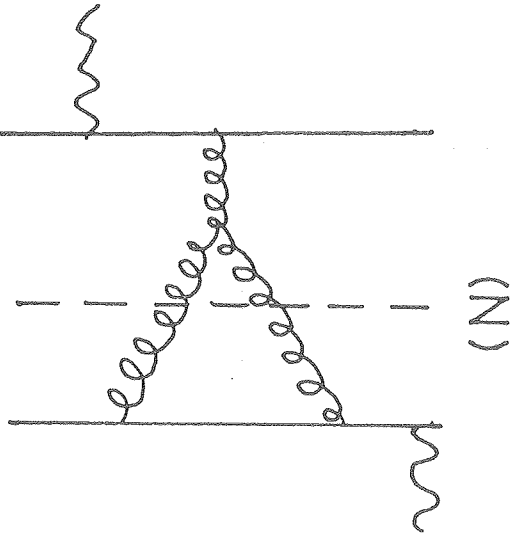
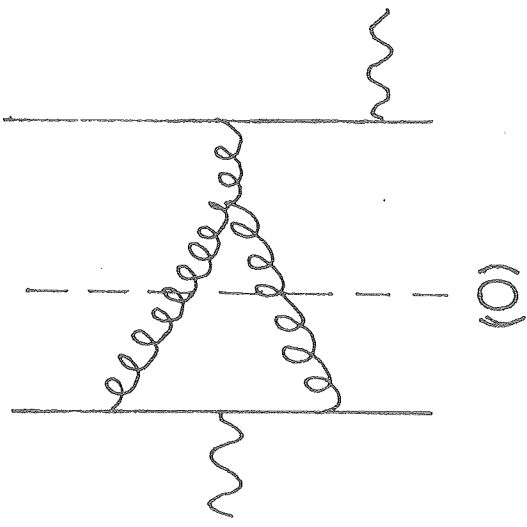


FIG.5 (CONT.)

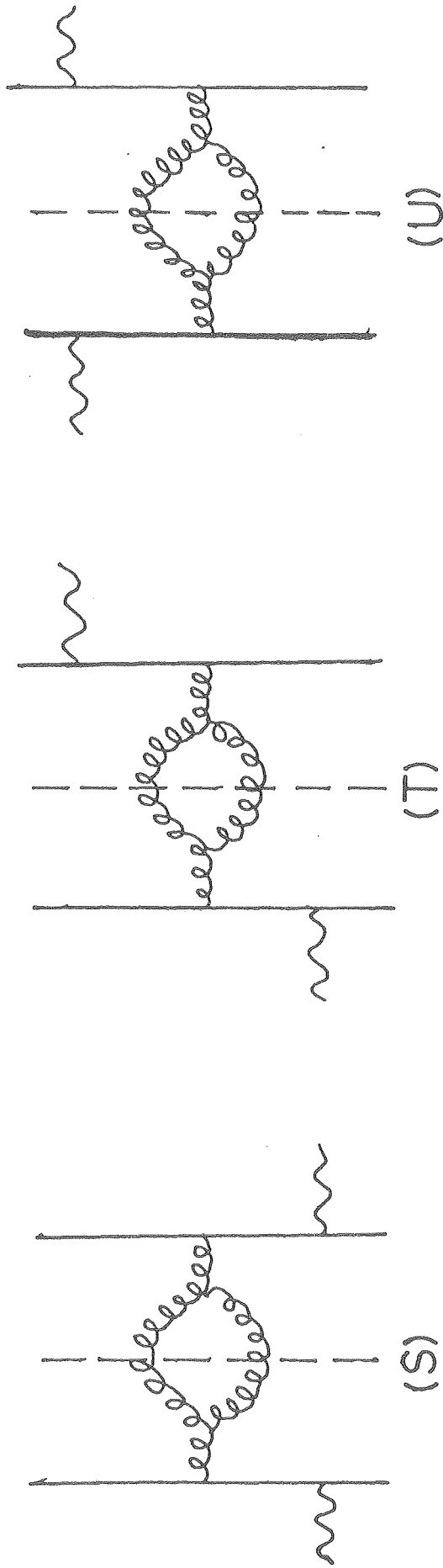


FIG. 5 (CONT.)

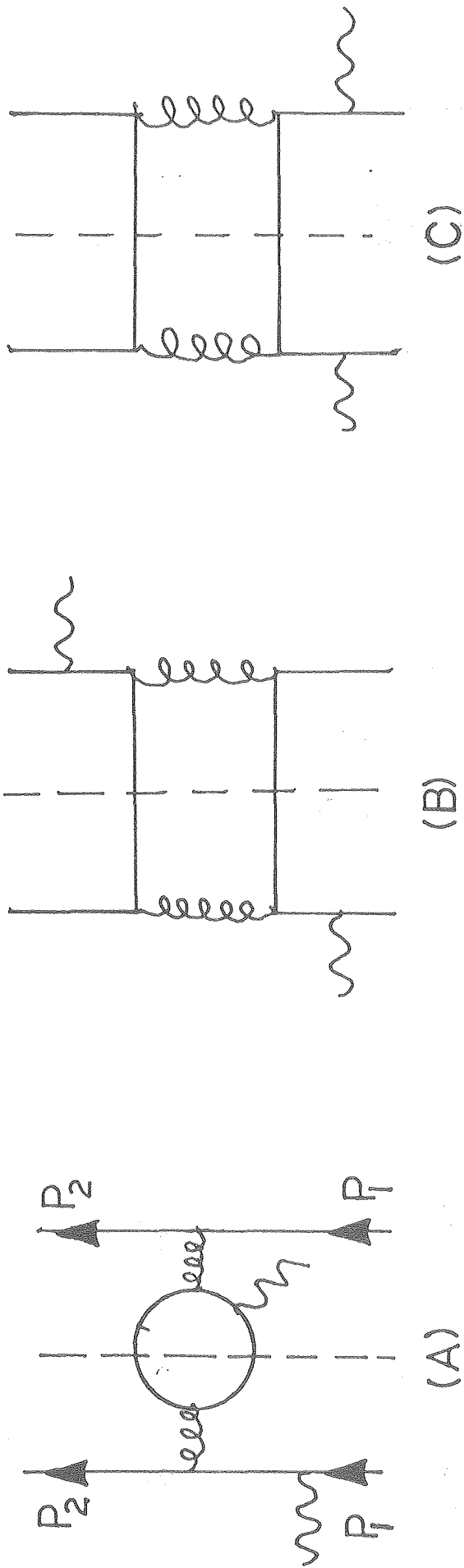
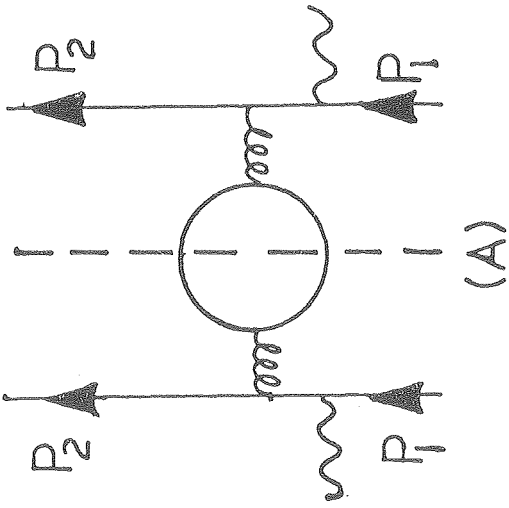
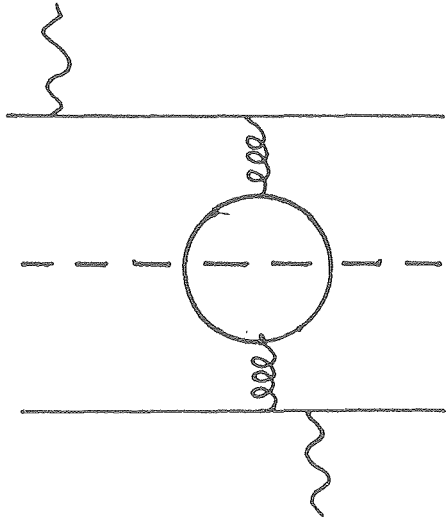


FIG. 6

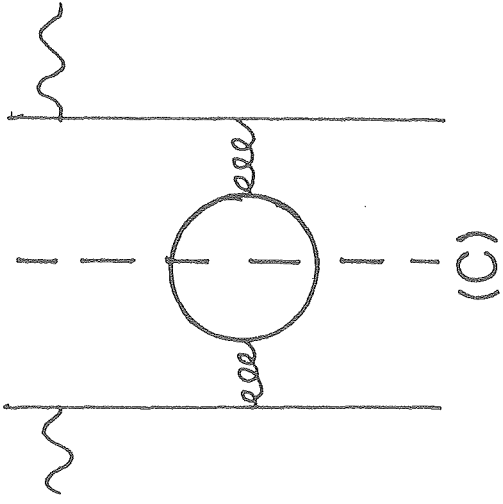


(A)

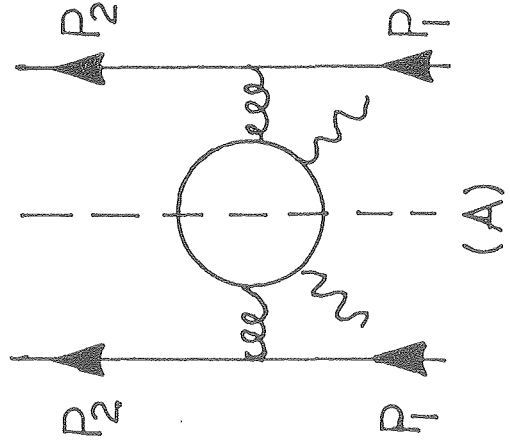


(B)

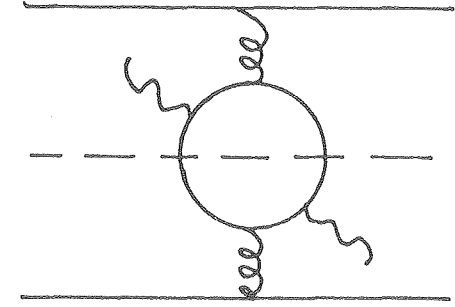
FIG. 7



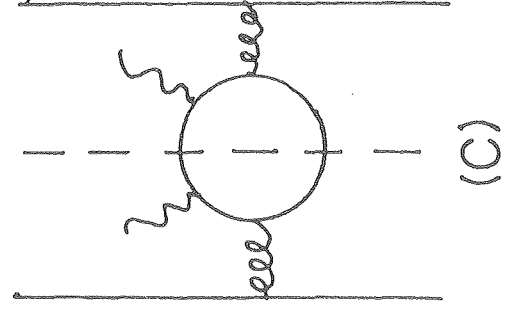
(C)



(A)

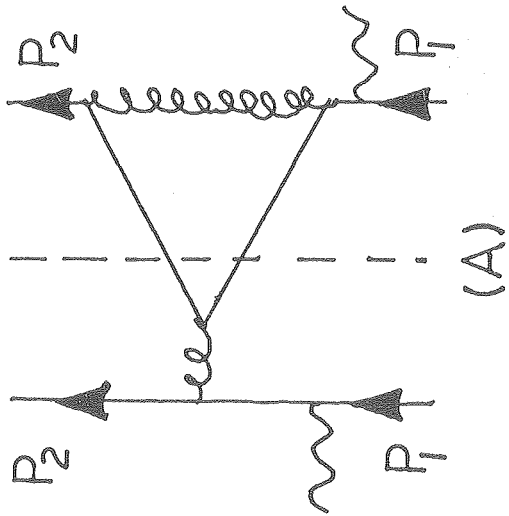


(B)

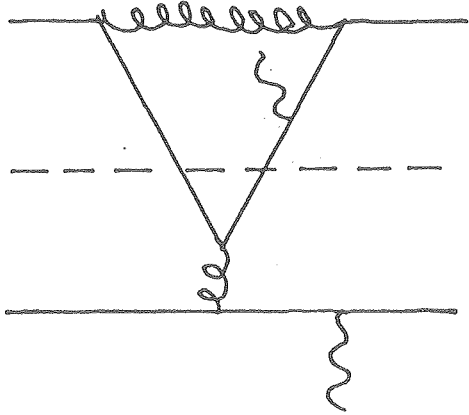


(C)

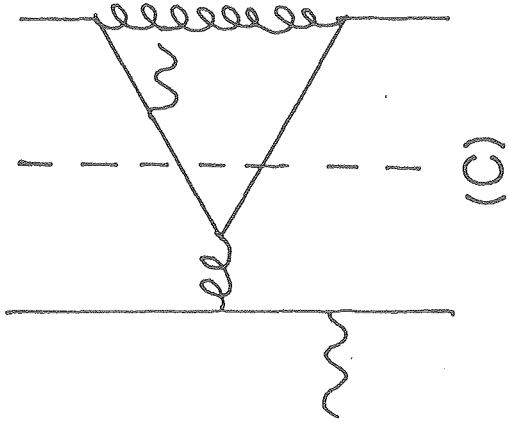
FIG. 8



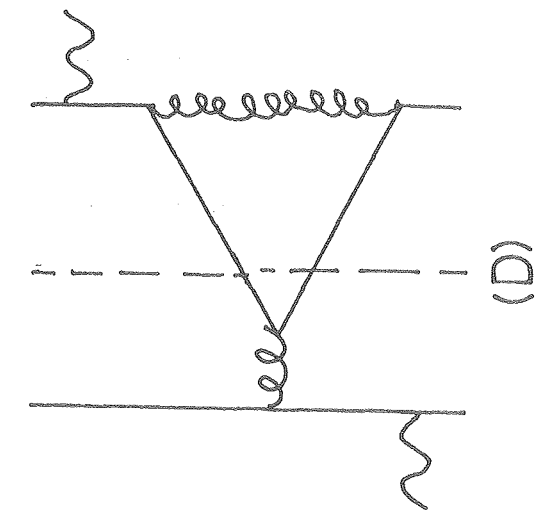
(A)



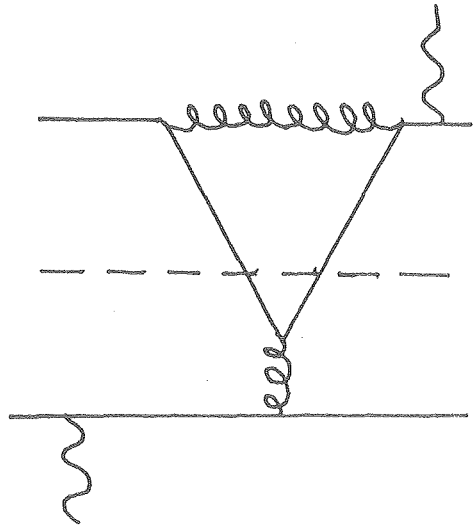
(B)



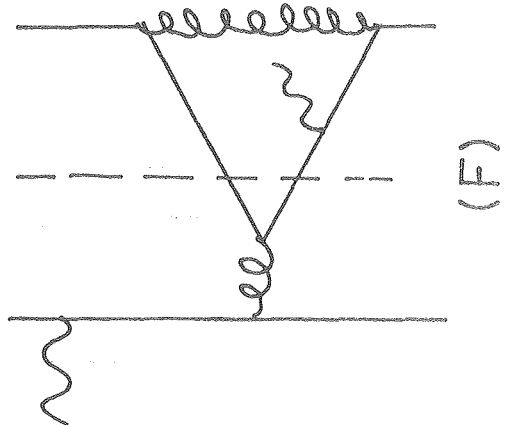
(C)



(D)



(E)



(F)

FIG. 9

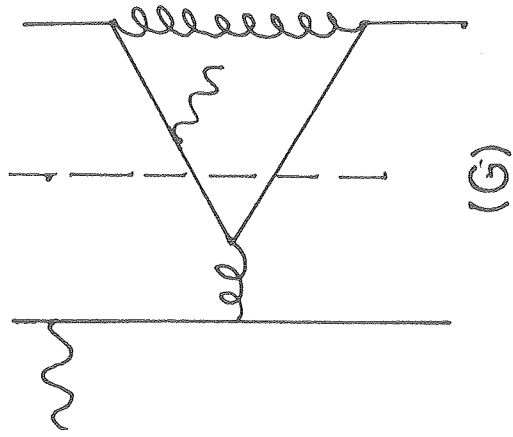
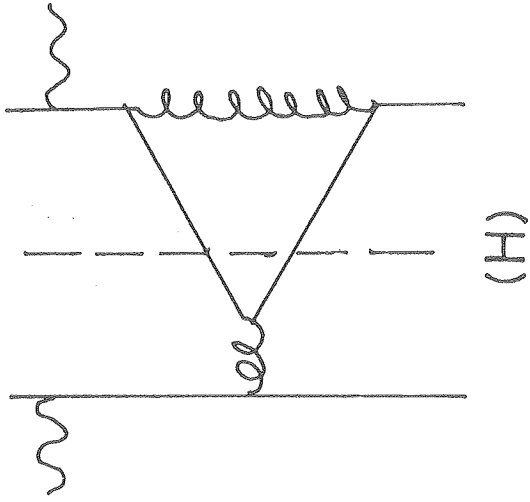


FIG. 9(CONT.)

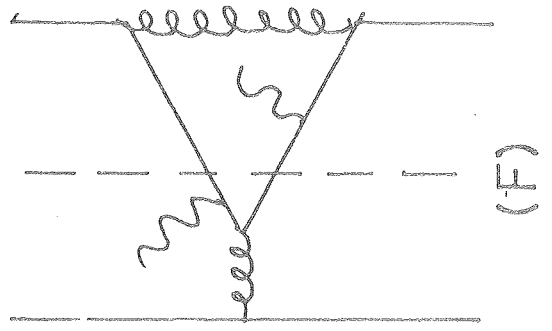
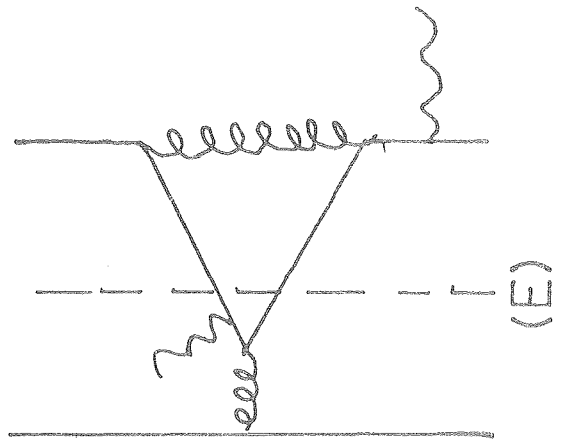
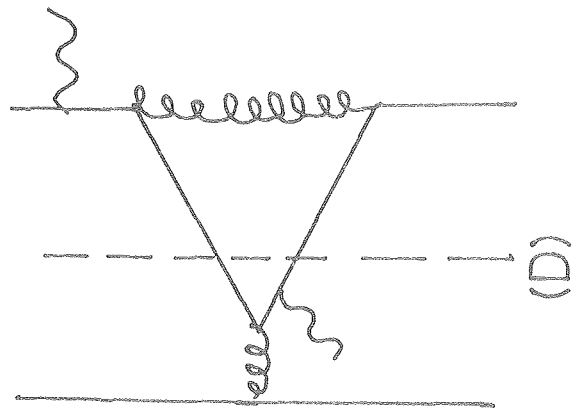
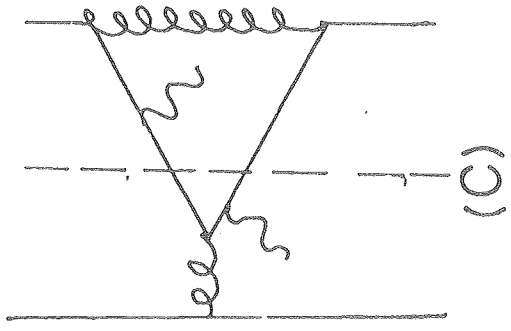
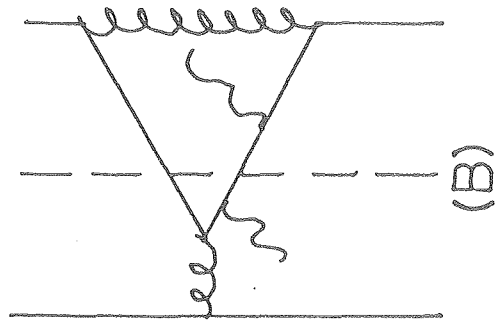
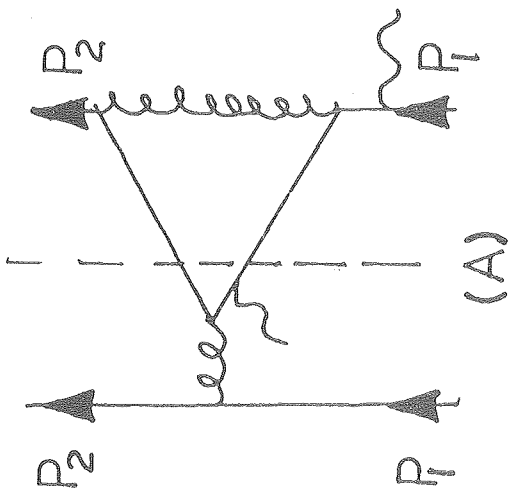
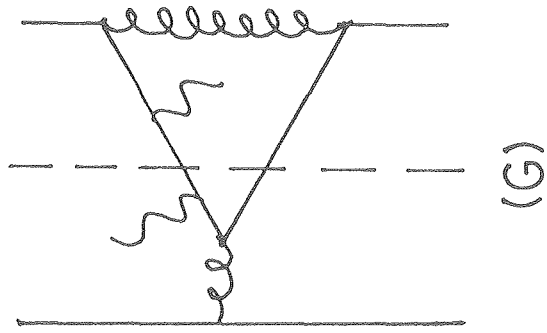
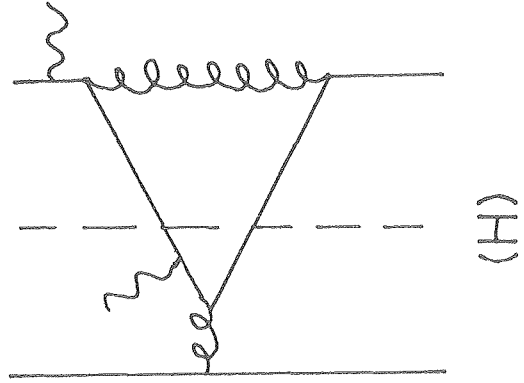


FIG. 10

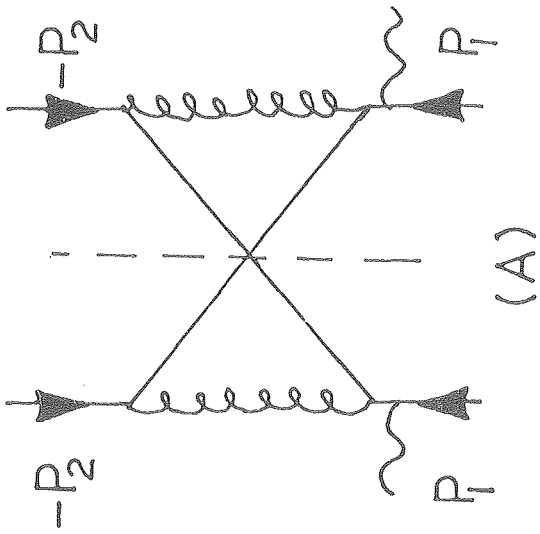


(G)

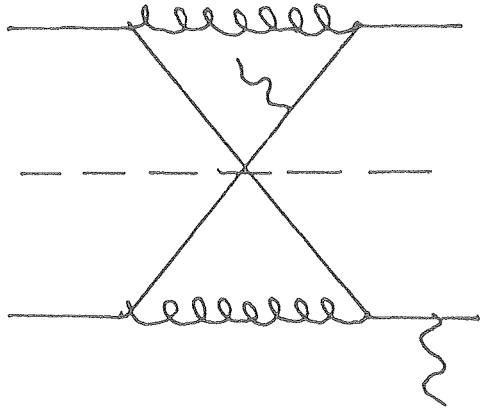


(H)

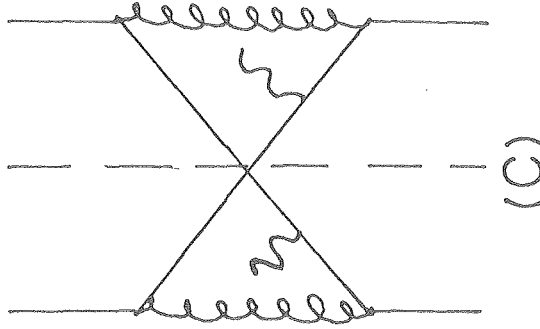
FIG. 10(CONT.)



(A)

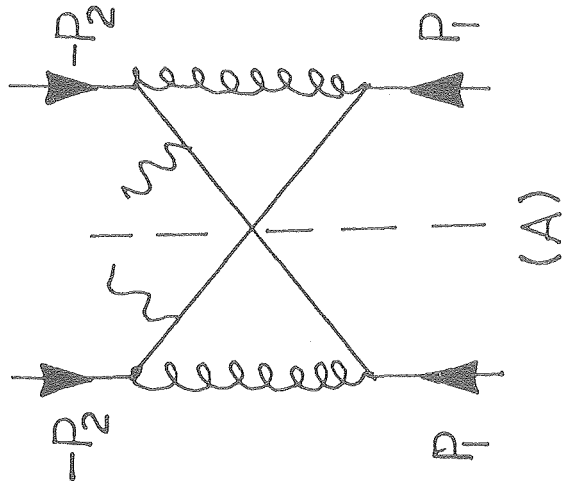


(B)

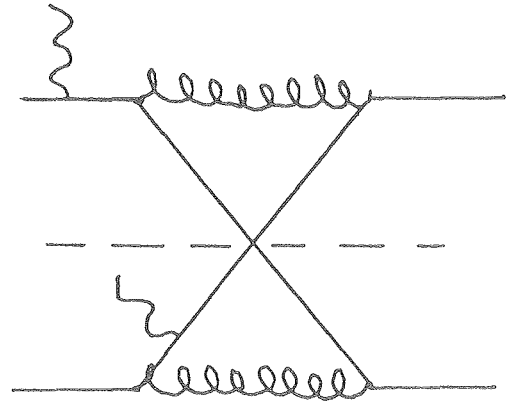


(C)

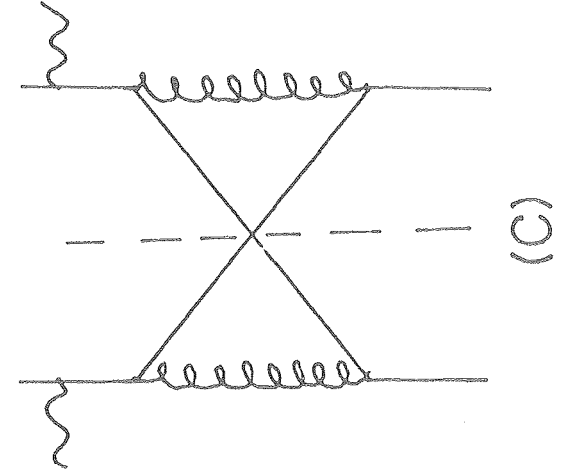
FIG. 11



(A)



(B)



(C)

FIG. 12

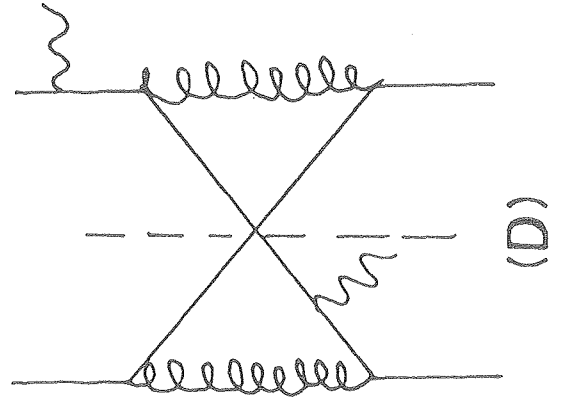
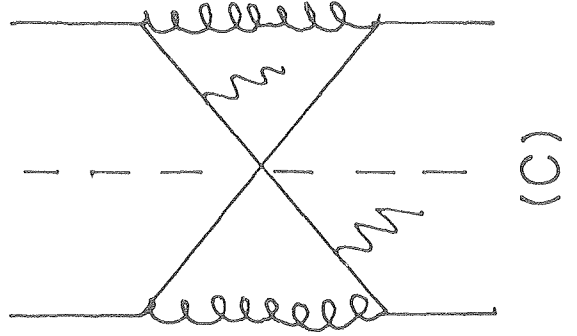
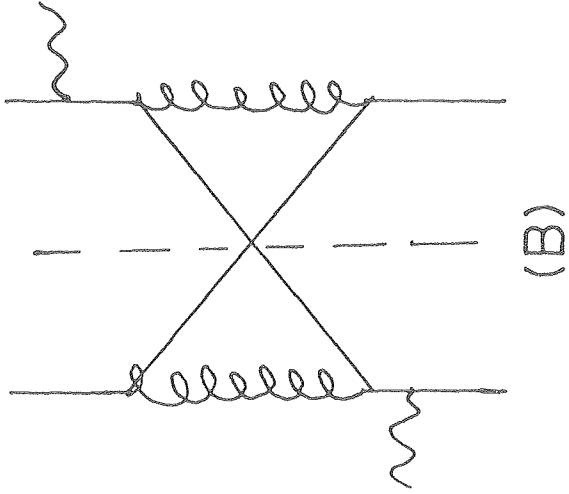
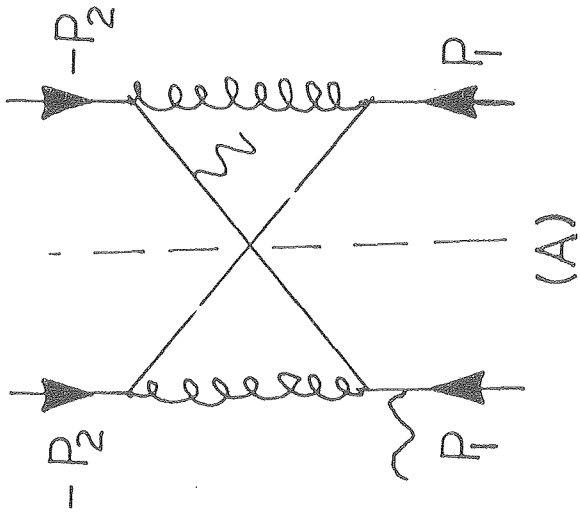


FIG. 13